Supplementary information

Surface-engineered PVDF-HFP/BNNS micro-nano fibers enable high-performance radiative cooling through synergistic photon scattering

Yuanxiang Xiao*[, a], Weishi Zheng[b], Jibiao Guan[c], Yingyao Chen[a], Runxin Chen[a], Yini Zhao[a], Shuangfei Xiang*[, c]

[a]Hangzhou Vocational and Technical College, Hangzhou 310018, China

[b]Zhejiang University School of Medicine, Hangzhou 310018, China

[c]School of Materials Science and Engineering, Zhejiang Sci-Tech University, Hangzhou 310018, China

Corresponding author, Email: xiaoyuan99998@yeah.net (Y. Xiao), xiang@zstu.edu.cn (S. Xiang)

1. FDTD numerical simulation

The impact of multiscale pores structures on the scattering property of PHB fabric was further explored theoretically by numerical simulation. To that end, finite difference time-domain (FDTD) solutions method was used here based on Lumbrical 2020R2.3 software. The scattering efficiencies of both multiscale pores and nanofibers were simulated across the solar wavelength of 0.25 ~ 2.5 μm. In the Mie theory framework, perfect matching layer (PML) boundary conditions were set and a scattering monitor was used. The full field scattering field (TFSF) optical source was selected to analyze scattering efficiencies in the wavelength range of 0.25 μm to 2.5 μm.

2. Calculation of the net cooling power

In an open environment, the material will emit heat through the surface, and the absorbed heat includes the heat from solar radiation (P_{solar}), ambient radiation (P_{amb}) and heat transfer by conduction and convection due to temperature differences ($P_{conv + cond}$). According to the heat balance analysis, the net cooling power (P_{net}) can be calculated as below:

$$P_{net} = P_{rad} - P_{amb} - P_{solar} - P_{conv + cond} \quad (1)$$

The P_{rad} is thermal radiation power from the emitter, which can be calculated by equation (2):

$$P_{rad} = 2\pi \int_0^{\frac{\pi}{2}} cos\theta sin\theta d\theta \int_0^{\infty} I_{bb}(T, \lambda)\varepsilon(\lambda,\theta)d\lambda \quad (2)$$

Where $2\pi \int_0^{\frac{\pi}{2}} cos\theta sin\theta d\theta$ is the integration over a hemisphere, T is the temperature covered by the sample, ε(λ, θ) is the emissivity of the material at the wavelength λ. $I_{bb}(T, \lambda)$ is the intensity of the radiation wave when the real-time temperature is T and the wavelength λ generated by the black body, which is calculated by equation (3):

$$I_{bb}(T, \lambda) = \frac{2hc^2}{\lambda^5} \frac{1}{e^{hc/\lambda K_B T} - 1} \quad (3)$$

Where h is Plank's constant, KB is the Boltzmann constant, c is the speed of light in a vacuum.

The P_{amb} represents the absorbed power from the atmosphere expressed by:

$$P_{amb} = 2\pi \int_0^{\frac{\pi}{2}} cos\theta sin\theta d\theta \int_0^{\infty} I_{bb}(T_{amb}, \lambda)\epsilon(\lambda,\theta)\varepsilon_{amb}(\lambda,\theta)d\lambda \quad (4)$$

T_{amb} is the ambient temperature and assumed to be 298.15 K, $\varepsilon_{amb}(\lambda, \theta)$ is the spectral directional emissivity of the sky atmosphere given by:

$$\varepsilon_{amb}(\lambda,\theta) = 1 - t(\lambda)^{\frac{1}{cos\theta}} \quad (5)$$

Where $t(\lambda)$ is the atmospheric transmittance at zenith angle θ and obtained from the MODTRAN software as the Mid-Latitude Summer Atmospheric Model.[1] θ is taken as 0° because our test device is completely facing the sun.

The P_{solar} represents the absorbed energy from the solar radiation expressed by:

$$P_{solar} = \int_{0.3\mu m}^{2.5\mu m} I_{solar}(\lambda)\varepsilon(\lambda,\theta)d\lambda \quad (6)$$

Where $I_{solar}(\lambda)$ is the ASTM G173 global solar intensity spectrum.

The lost energy due to convection and conduction ($P_{conv+cond}$) expressed by:

$$P_{conv+cond} = h_{nr}(T_{amb} - T) \quad (7)$$

Where h_{nr} is non-radiative coefficient related to environmental conditions.

3. Outdoor thermal management test

The fabric (5×5 cm^2) was placed on an insulation foam box that was covered with aluminum foil to reduce heat transfer through conduction and radiation from the ambient. The real-time temperature was monitored using a thermocouple that was put underneath the fabric and collected by a data recorder. During the test, the whole device was sealed with low-density polyethylene (PE) film to prevent heat convection from the surroundings and ensure negligible heat loss. The solar irradiance was recorded by a solar power meter (TES-1333R). Relative humidity was measured by the humidity datalogger (TH21R-EX). The wind speed was measured using a digital anemometer (AS 856).

4. Wearing comfort evaluation

The water vapor permeability (WVP) determines the comfort of the fabric when dressed. The value of WVP was evaluated by the ASTME-96 standard test method. The fabric was sealed in a glass bottle containing a certain amount of distilled water at 25 °C for 24 h, and then the WVP was calculated as equation (8):

$$WVP = \frac{G}{t \times A}(g/h/m^2) \quad (8)$$

Where G (g) is the weight change of the distilled water after 24 h, t is the test time (h) and A (m^2) is the test area. Three samples were tested and their mean was reported.

The air permeability of the fabric was measured with an air-permeability tester (YG461E, Wenzhou Fangyuan Instrument Co., Ltd., China) following the GB/T 24218.15-2018 standard.

The tensile strength of the sample was tested by Tensile Machine (Dongguan A-Pex Test Equipment Co. Ltd. China, model: AP-8008-600N) according to the ISO 13934-1-1999 Textiles - Tensile properties of fabrics - Part 1: Determination of maximum force and elongation at maximum force using the strip method. The fabric (rectangle shape, 200 mm × 50 mm) was stretched at a constant rate of 100 mm/min, three samples were tested under the same conditions, and their mean was reported.

The laundering durability of the fabric sample was tested according to AATCC 61-

2006(2A) standard method. Fabric (5 cm × 5 cm) was washed in stainless steel (NO. 50) washing tank containing detergent (soap, without fluorescent brightening agent) with a concentration of 0.15 % (w/v) at 49 ± 2 °C with a rotating speed of 40 rpm. After 45 min, the sample was taken out, then washed and dried. One machine washing cycle is equivalent to five home washings.

5. Biosafety performance test

5.1. Cell viability test

The cell viability of the fabric to L929 cells (mouse fibroblasts) was detected by cell counting kit 8 (CCK-8) following the ISO 10993-5: 2010 (Part 5: Test for in vitro cytotoxicity) standard method. Fabrics (5 × 5 cm^2) were immersed in a phosphate buffered saline (PBS) solution (37 °C, 100 mL) for 24 h. The filtered leachate solution was sterilized by high temperature and high pressure. L929 cells (10^4 mL^{-1}) were inoculated on a 96-well plate (100 $\mu L \cdot well^{-1}$) with high-sugar DMEM medium with 10 % FBS and cultured at 37 °C with 5 % CO_2 for 24h. And then carefully remove the DMEM medium and replace it with the leachate (100 μL, diluted 50-fold in DMEM). After co-culturing for 24 h, removing the leachate and replace it with 100 μL of FBS-free medium containing 10 μL of CCK-8 reagent. Incubate at 37 °C for 2 h, The absorbance of the sample was detected by a microplate reader (Epoch2, Bio-Tek) at a wavelength of 450 nm. PBS solution served as the blank control.

5.2. Live-dead cell staining test

Fabrics (5 × 5 cm^2) were immersed in a PBS solution (37 °C, 100 mL) for 24 h. The filtered leachate solution was sterilized by high temperature and high pressure. L929 cells (5×10^4 mL^{-1}) were inoculated on a 24-well plate (500 $\mu L \cdot well^{-1}$) with high-sugar DMEM medium with 10 % FBS and cultured at 37 °C with 5 % CO_2 for 24h. And then carefully remove the DMEM medium and replace it with the leachate (500 μL, diluted 20-fold in DMEM). After co-culturing for 24 h, the leachate was gently aspirated, and the wells were washed once with PBS. Subsequently, the cells were stained for viability and cytotoxicity using 0.2% Calcein-AM and Propidium Iodide (PI). After a 15 min incubation, the cells were observed under a fluorescence microscope.

5.3 Skin stimulation test

The skin safety test of PHB-4% fabric was carried out on rats following the ISO 10993-10: 2010 (Part 10: Test for irritation and skin sensitization) standard method. Before testing, rats were left for a week under controlled conditions (12 h light/dark cycles at 20–26 °C) for acclimatization. The hairs of rats on the back (3 cm × 3 cm) were removed without damaging the skin. After disinfecting the area with iodophor, a wound with a diameter of 1 cm was cut with a scalpel. The wound was then treated with a saline cotton ball to stop bleeding. The original cotton fabric was employed as a control sample. Two rat skin areas were covered with the original cotton and PHB-4% fabrics for 24 h, respectively. Then, the fabric was removed, and photographs were taken of the rat skin to observe erythema and edema using the naked eye.

In addition, after the damaged skin of the rats was covered with fabrics for 24 h, the fabrics were removed, and the skin epithelial cells were extracted to analyze morphological changes. Subsequently, rat skin samples were paraffin-embedded, sectioned, and stained with hematoxylin and eosin (H&E). The stained tissue sections were observed using light microscopy (Olympus BX51) for standard histological analysis.

All the experiments in the skin test were performed in compliance with the laws and guidelines by the Department of Science & Technology of Zhejiang Province (China), and their committees have approved the experiments.

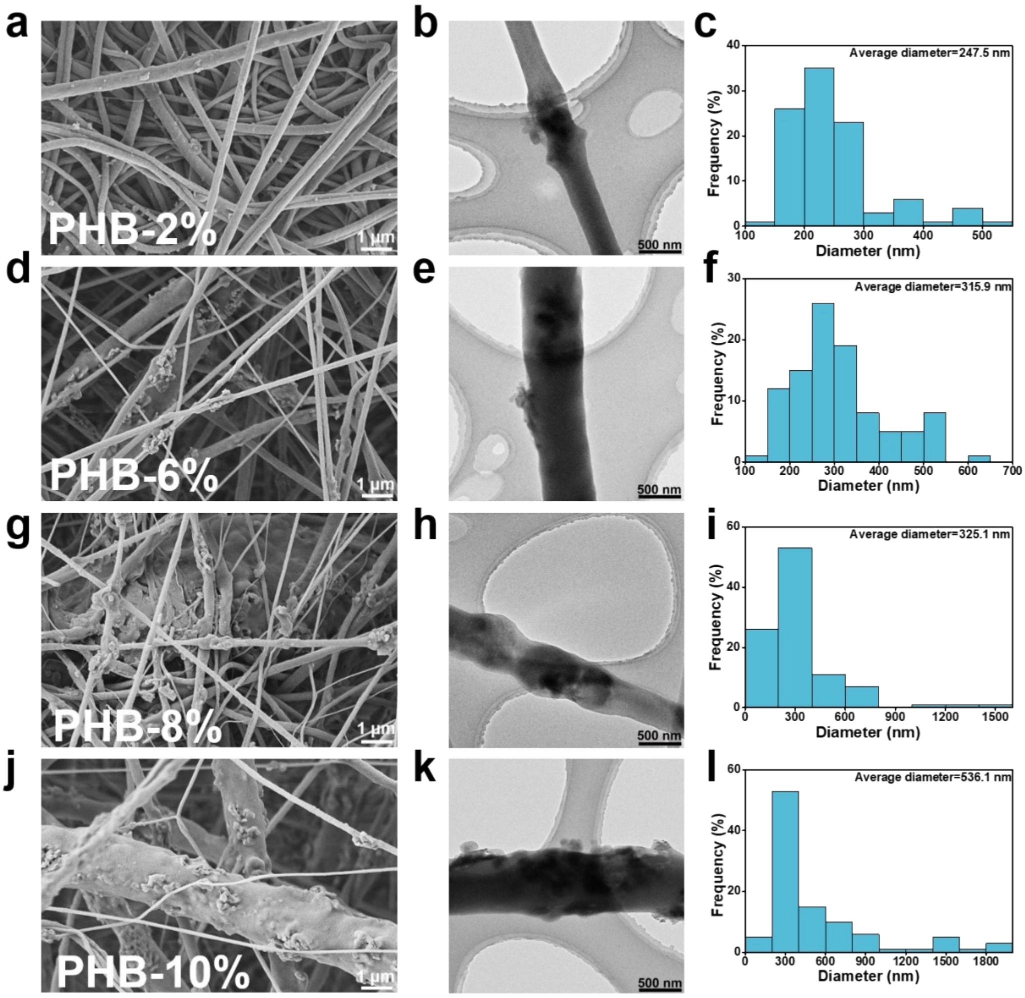

Fig. S1. SEM, TEM, and diameter distribution images of PHB-2% (a, b, c), PHB-6% (d, e, f), PHB-8% (g, h, i), and PHB-10% (j, k, l) fabrics.

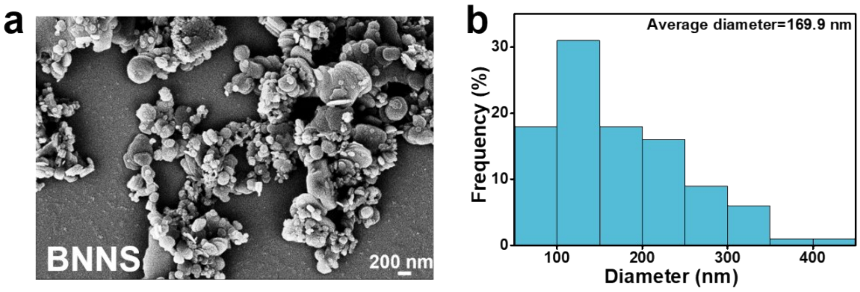

Fig. S2. SEM image (a) and diameter distribution (b) of BNNS.

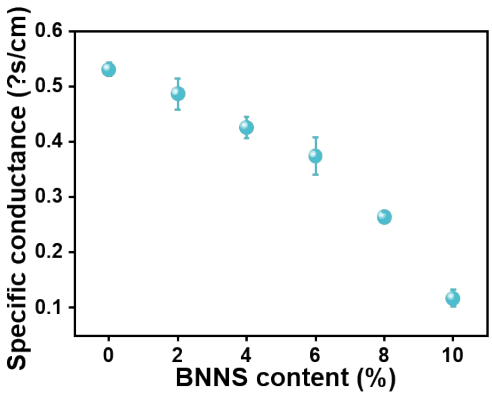

Fig. S3. The specific conductance of PVDF-HFP solution with different BNNS content.

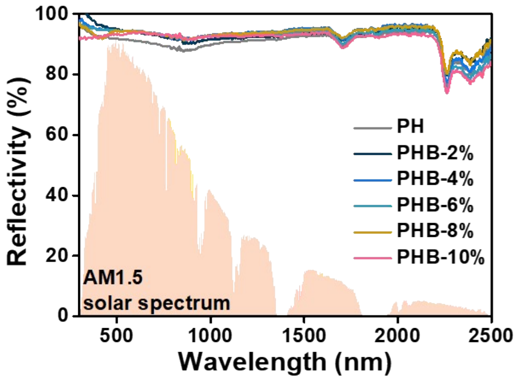

Fig. S4. The solar reflectivity spectra of the fabrics with different BNNS content.

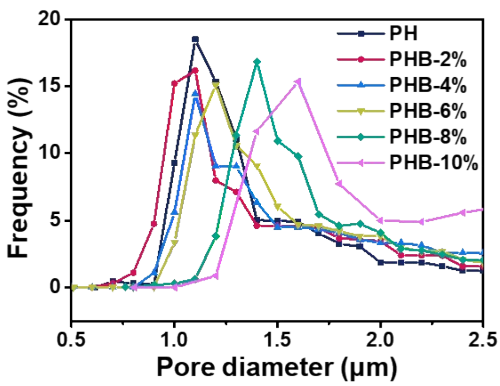

Fig. S5. Pore diameter distribution of the fabrics with different BNNS content.

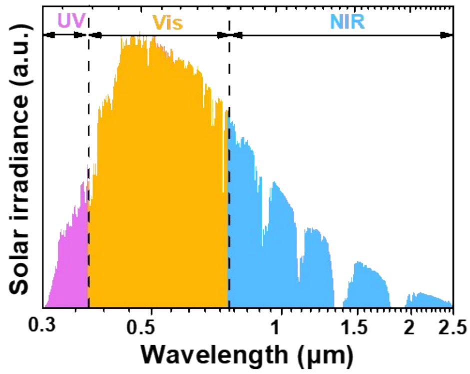

Fig. S6. Spectra of solar irradiation (plotted by AM 1.5G, global tilt).

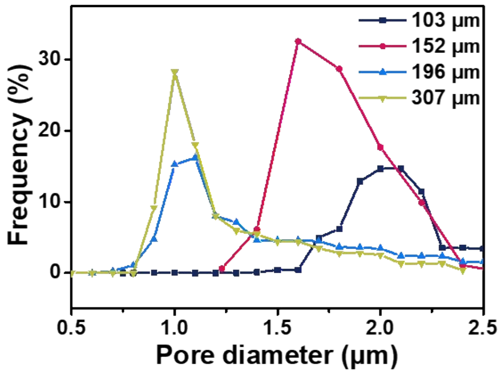

Fig. S7. Pore diameter distribution of the PHB-4% fabrics with different thickness.

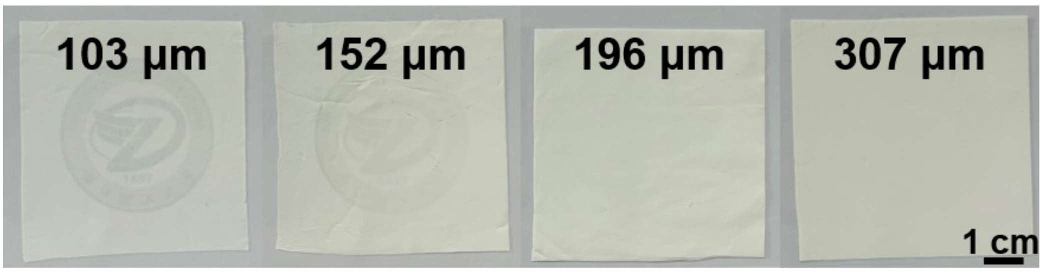

Fig. S8. Optical pictures of PHB-4% fabrics with different thickness.

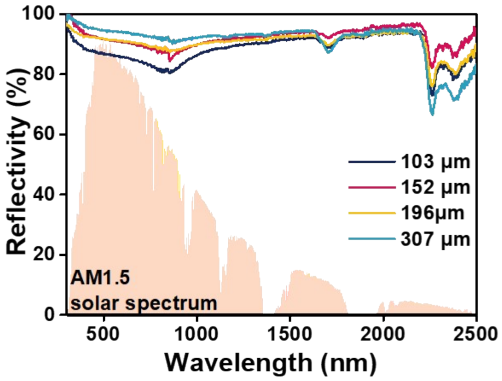

Fig. S9. The solar reflectivity spectra of the PHB-4% fabrics with different thickness.

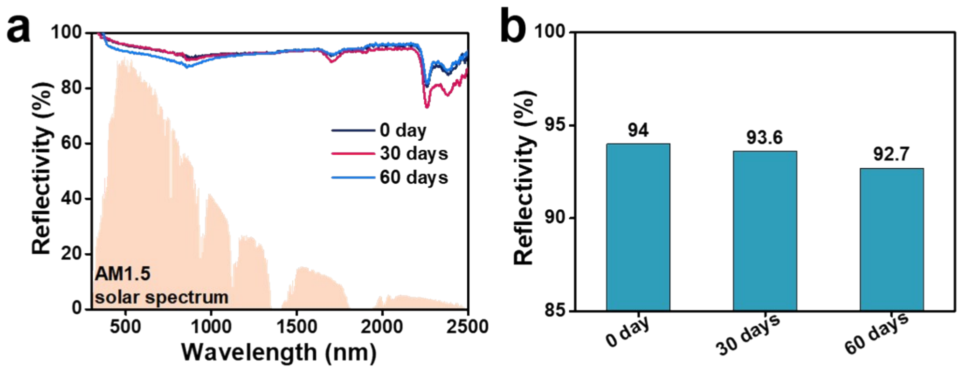

Fig. S10. The solar reflectivity spectra (a) and calculated value (b) of the PHB-4% fabric under direct sunlight for different days.

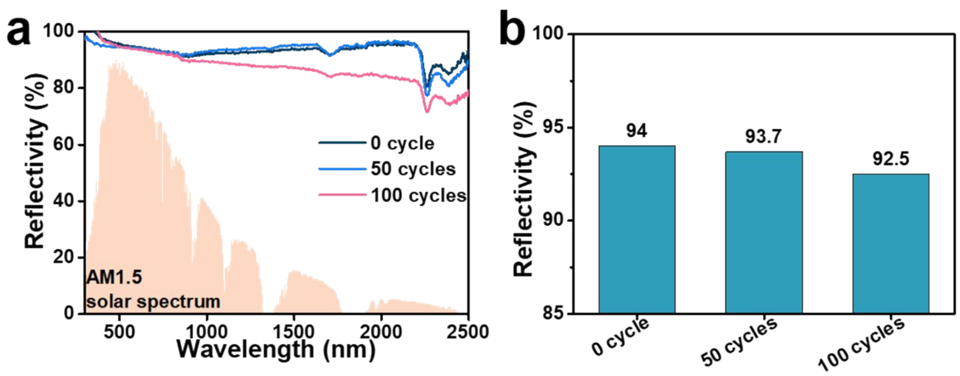

Fig. S11. The solar reflectivity spectra (a) and calculated value (b) of the PHB-4% fabric undergo difference washing cycles.

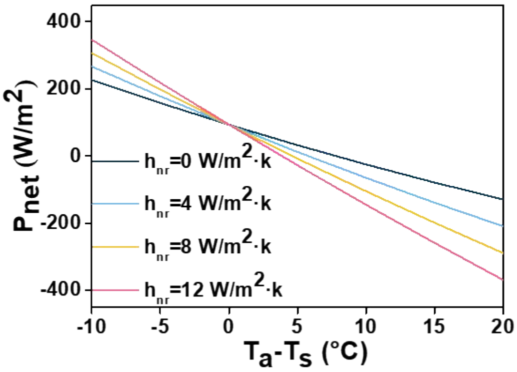

Fig. S12. Calculated P_{net} value of PHB-4% fabric.

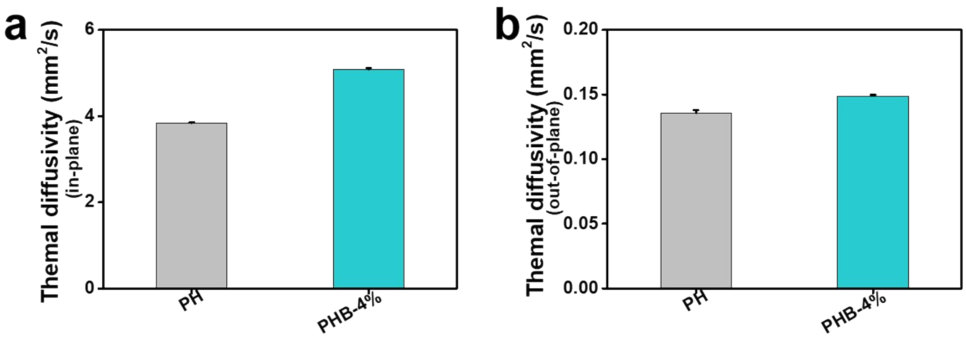

Fig. S13. (a) In-plane and (b) out-of-plane thermal diffusivity of PH and PHB-4% fabrics.

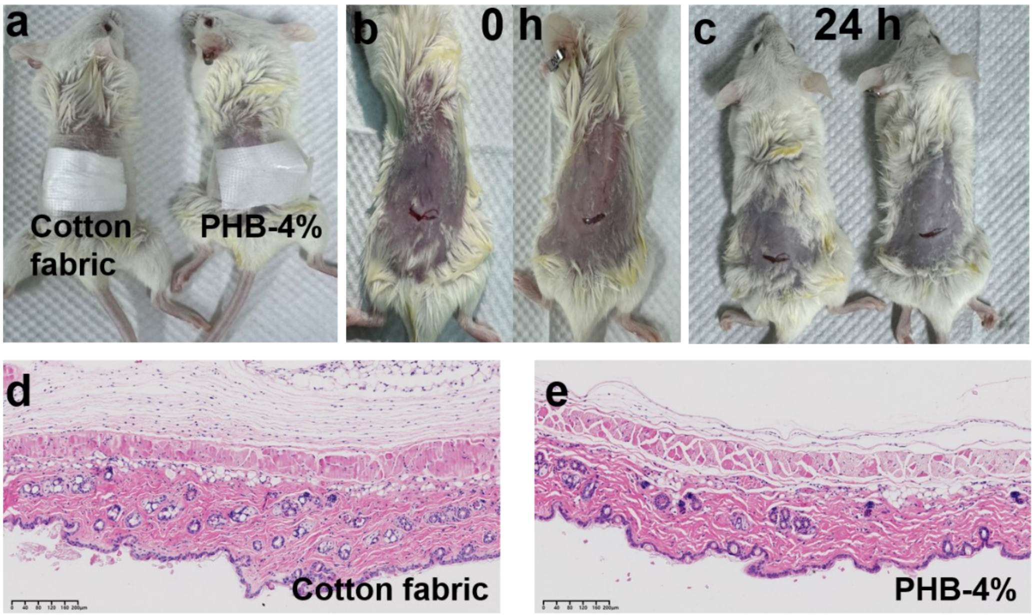

Fig. S14. Skin stimulation tests with applied fabrics adhered to rat skin for 24 h (left wound: cotton fabric, right wound: PHB-4% fabric) (a-c). Hematoxylin and eosin staining images of skin collected from different groups of rats: cotton fabric (d) and PHB-4% (e). Scale bar: 200 μm.

Reference

1. S. S. Shen, A. Berk, P. E. Lewis, G. P. Anderson, P. K. Acharya, L. S. Bernstein, L. Muratov, J. Lee, M. Fox, S. M. Adler-Golden, J. J. H. Chetwynd, M. L. Hoke, R. B. Lockwood, J. A. Gardner, T. W. Cooley, C. C. Borel, P. E. Lewis and E. P. Shettle, presented in part at the Algorithms and Technologies for Multispectral, Hyperspectral, and Ultraspectral Imagery XII, 2006.